Mechanical Recovery of Dentin Following Remineralization In Vitro – an Indentation Study

Luiz E. Bertassoni, **Stefan Habelitz**, **Sally J. Marshall**, and **Grayson W. Marshall**
Division of Biomaterials and Bioengineering, Department of Preventive and Restorative Dental Sciences, University of California, San Francisco, San Francisco, CA 94143-0758

Abstract

This study sought to gain insights into the steps leading to remineralization and mechanical recovery of hydrated dentin. Mechanical recovery in water was hypothesized to result from effective mineral matrix binding and to occur from the innermost regions outwards due to increased number of nucleation sites. Partially demineralized (0.05 M acetate, pH=5.0, 8 hrs) dentin was remineralized using calcium and phosphate solutions of 10.1 or 9.8 degree of saturation (DS) for hydroxyapatite (pH=7.4) for 4, 8 or 24 hours. Remineralization used a constant solution composition approach, which allowed for a continuous mineral growth with relatively constant thermodynamic driving forces. Rates of crystal growth rates (R) were calculated using concentrations of calcium and phosphate. Before and after de- and remineralization specimens had their surface and cross-section elastic moduli measured using AFM-nanoindentation in water. DS=10.1 provided higher R and higher mechanical recovery at the surface (p<.0001). Cross-sectional measurements showed that subsurface mechanical recovery occurred from the innermost demineralized areas gradually outwards for both groups with no statistical differences at different DS, thus suggesting that remineralization is driven by mineral growth within nucleation sites with preserved collagen fibrils. Further, mechanical recovery appeared to initially obey a heterogeneous pattern which vanished with time. This study provides evidence of mechanical recovery of hydrated dentin after remineralization and novel insights into the steps leading to mechanical recovery of carious dentin.

Keywords

Dentin; remineralization; mechanical properties; nanoindentation; caries

1. Introduction

In dental caries, oral bacteria generates acids that diffuse into enamel and further into dentin, the most abundant mineralized tissue in the tooth, dissolving mineral, and eventually destroying the matrix. As a result of this process the mechanical properties of the affected tissues are significantly decreased. Current remineralization treatments aim at restoring the function of the affected tissues, however, to date little information exists regarding the steps

Conflict of interest statement
The authors have no conflict of interest.

leading to mechanical recovery of dentin, particularly in physiologic conditions of hydration.

Dentin is composed of about 30 vol % type I collagen fibrils and noncollagenous proteins that form a scaffold reinforced with apatite, which represents 50% of the matrix, with the remainder being fluids (Marshall et al., 1997). The apatite occurs in two compartments: extrafibrillar mineral, in the spaces separating the fibrils (Katz and Li, 1973), and intrafibrillar mineral, within the fibrils (Landis et al., 1993). It has been suggested that remnant intrafibrillar mineral crystallites that are present within the collagen after partial demineralization of dentin (Balooch et al., 2008) might act as sites for apatite nucleation and re-growth thus facilitating remineralization and recovery of the mechanical properties (Kinney et al., 2003a).

Testing of the mechanical properties of mineralized tissues in water, in general, appears to be critical to obtain information about the association of mineral with the organic components that form their matrices (Angker et al., 2004; Bembey et al., 2006; He and Swain, 2007; Marshall et al., 2001; Oyen, 2008; Rho and Pharr, 1999). This is particularly significant in measurements of remineralization of dentin (Bertassoni et al., 2009), where it is hypothesized that improved mechanical recovery occurs when the mineral is effectively re-associated with the organic matrix and little mechanical recovery is expected when mineral is regained but poorly attached to the matrix.

Several approaches have been reported in an effort to remineralize dentin, including the use of carboxylic acid-containing polyelectrolytes (Tay and Pashley, 2008), phosphoproteins (Saito et al., 1998), casein phosphopeptide-amorphous calcium phosphate (Rahiotis and Vougiouklakis, 2007), colloidal nano-beta-tricalcium phosphate (Shibata et al, 2008) and bioactive glass particles (Vollenweider et al., 2007), all claiming relative success with respect to the observation of mineral forming at the lesion site. However, to date it has not been demonstrated that the mechanical properties of dentin recover after remineralization to its sound values when tested in water, which is critical considering that dentin is naturally hydrated tissue.

In this study, we sought to gain insights into the steps leading to mechanical recovery of dentin in water following calcium and phosphate remineralization treatments. To accomplish this we studied the mechanical properties of the surface and cross-section of simulated caries lesions in water after remineralization using solutions of relatively higher (10.1) or lower (9.8) degrees of saturation (DS) with respect to hydroxyapatite. We hypothesized that mechanical recovery should occur gradually from the innermost regions outwards with remineralization due to increased presence of active nucleation sites.

2. Materials and Methods

Dentin specimen preparation and demineralization

Permanent human third molars were obtained according to protocols approved by the UCSF Committee on Human Research. Teeth were sterilized and stored in de-ionized water and thymol at 4°C. Dentin blocks (3.5 mm × 3.5 mm × 2 mm) were cut from the mid-coronal region of the teeth with the exposed surface perpendicular to the tubule direction. The specimens were ground with SiC abrasive papers down to 1200 grit and polished with diamond suspensions (Buehler, Lake Bluff, IL) of 1.0 and 0.25 μm. Each specimen surface was half covered with a masking tape to provide a reference area of normal dentin, and the remaining surfaces were exposed to a demineralizing solution containing 0.05 M acetate buffer and 2.2 mM calcium phosphate plus 0.1% thymol (McIntyre et al., 2000) and adjusted to pH 5.0 to create lesions approximately 30 μm deep.

Remineralization experiments

Remineralization experiments used the constant solution composition method first described by Tomson and Nancollas (1978). In this method a main mineralizing solution is controlled by a pH meter; the addition of specimens induces precipitation of hydroxyapatite, thus resulting in free H^+ ions in solution (Eq. 1) and yielding a pH drop.

$$5Ca^{2+}+3HPO_4^{2-}+H_2O=Ca_5(PO_4)_3OH+4H^+$$

(Eq. 1)

The drop in pH (below 7.4) triggers the simultaneous addition of two titrant solutions with concentrations that compensate for the ions precipitated according to calculations of mass balance described elsewhere (Koutsoukos et al., 1980). The basic set up of the constant composition system is shown in Fig 1.

Groups were divided according to the degree of saturation (DS) of the remineralizing solution used, being either relatively higher (10.1) or lower (9.8). DS was calculated as equal to $pK_{sp} - pIP$, where pK_{sp} is the negative logarithm of the solubility activity product of hydroxyapatite and pIP is the negative logarithm of the ionic activity product. Software developed by M. J. Larsen (2001) has been applied for calculating DS. DS values were based on concentrations of calcium and phosphate obtained by means of a calcium selective electrode and a spectrophotometer (Milton Roy, Genesys 5, Ivyland, PA, USA), respectively. Groups and remineralizing solution's compositions are described in Table 1. A minimum of 4 experiments was performed per group. Each experiment used 3 specimens, with one specimen removed at 4, 8 or 24 hours.

Additionally, the rates of crystal growth (R) were calculated to determine the amount of mineral precipitated per experiment at different time points according to equation 2

$$R=\frac{C_{eff}}{S_A}\frac{dV}{dt}$$

(Eq. 2)

where C_{eff} is the equivalent number of moles precipitated per liter of added titrant, dV/dt is the titrant curve gradient and S_A is the surface area available for crystals to grow, in this case the area comprising the surface of demineralized region (half the specimen's surface).

AFM Nanoindentation

Specimens were stored dry and rehydrated for at least 1 hour prior to indentation tests. Indentations were done with specimens immersed in de-ionized water using a Berkovich indenter on an atomic force microscope (Nanoscope III Digital Instruments, Santa Barbara, CA, USA/Hysitron Inc., Minneapolis, MN, USA) to obtain values of reduced elastic modulus (E_r). Indentations were performed with loading and unloading times of 3 seconds down to a depth of 500 nm with a 10 second holding period. Each indentation yielded a load-deformation curve, from which the E_r was determined according to equation 3 (Doerner and Nix, 1986)

$$E=\frac{\sqrt{\pi}}{2\sqrt{a}}S$$

(Eq. 3)

where *S* represents the slope of the unloading curve based on the method of Oliver and Pharr (Oliver and Pharr, 1992) and *a* is the indentation contact area. In all cases, hardness values that were also obtained for each indentation strictly correlated with values of elastic modulus, and thus they were not included for the sake of brevity. Indentations were always positioned in the intertubular region, avoiding tubules and peritubular dentin. Measurements were divided in two steps. Initially, 5 specimens had both their normal (masked) and lesion (unmasked) surfaces measured and the data was used as baseline. After remineralization specimens from each treatment group had a minimum of 15 indentations performed on the surface of the lesion area that was prepared to lie perpendicular to the tubule direction. Secondly, the specimens were embedded, cross-sectioned and polished following protocols described above. Two lines containing 15 indents each were positioned along 45 μm, parallel to the tubule direction, starting at the outermost regions of the cross-sectioned teeth and moving inward at intervals of 3 μm. Surface measurements were averaged and analyzed using a mixed effects regression model followed by pair-wise comparisons of treatments and time within treatments. Cross-section data was analyzed using ANOVA followed by a Tukey's test with a significance level of 5% to compare values of each distance point between groups.

3. Results

Remineralization experiments

Experimental conditions are reported in Table 1. Only minor variations in concentration and pH were noted, thus thermodynamic conditions were maintained in close proximity to the values initially set. As expected, growth rates (*R*) increased with time and were higher for group DS=10.1 (Fig. 2). Additionally, the increase in *R* obtained with both DS=10.1 and 9.8 became less significant at each time point.

AFM Nanoindentation

Surface mechanical recovery—Figure 3 shows the values of E_r of groups DS=10.1 and 9.8 as well as the lesion baseline values and normal dentin groups. Graphs depict surface (Fig 3a) and cross-section measurements after 4 (Fig. 3b), 8 (Fig. 3c) and 24 hrs (Fig. 3d). Surface measurements showed that DS=10.1 had a significantly higher E_r than the demineralized and DS=9.8 groups after 8 and 24 hours (p<.0001). Yet, the surface recovery achieved with both treatments was always significantly lower than the values of normal dentin (p<.0001).

Cross-section mechanical recovery—Cross-sectional measurements showed that DS=10.1 and DS=9.8 provided E_r values that generally were not statistically different from each other, regardless of the distance from the surface. Results also revealed that demineralization resulted in a gradient in properties that increased gradually from the outermost regions inwards, whereas remineralization recovered the properties from the innermost regions gradually outwards. Comparisons between treatment groups showed that after 4 hours DS=10.1 had significantly higher values than the demineralized dentin within 9 μm from the surface and reached values similar to normal dentin within 21 μm (p<.0001). DS=9.8, on the other hand, had values significantly higher than demineralized dentin within 9 μm from the surface and reached values of normal dentin within 15 μm (p<.0001). After 8 hours DS=10.1 provided significantly higher values than the demineralized dentin within 3 μm (p<.0001) from the surface and values similar to normal dentin within 18 μm (p<.001), whereas DS=9.8 was higher than demineralized dentin within 6 μm (p<.05) and reached values of normal dentin at 21 μm (p<.05). Finally, after 24 hours, both solutions produced values higher than the demineralized group within 3 μm from the surface (p<.0001), whilst

properties similar to normal dentin were obtained within 12 (p<.0001) and 18 μm (p<.01) from the surface for DS=10.1 and DS=9.8 respectively.

4. Discussion

This study sought to gain insights into the steps leading to remineralization of dentin by evaluating the mechanical recovery of simulated caries lesions in water after remineralization with calcium phosphate solutions of DS=10.1 and 9.8. In the following discussion we will address the testing methods, the steps leading to mechanical recovery, the process and pattern of remineralization and offer a model for remineralization at the nano- and micro-structural levels.

Mechanical recovery of remineralized dentin in water

To date, the effectiveness of remineralization of dentin has been mostly determined by measurements of mineral content (Arends et al., 1997; Bertassoni et al., 2009). The so-called "quality of dentin", however, is dependent upon the sum total of characteristics of the tissue that influence its competence: microstructure, mineral density and the location of the mineral within the organic matrix (Bertassoni et al., 2009). In contrast to measurements of mineral density, mechanical properties values integrate all of these factors, since tissue strength is determined by mineral content, architecture and, in water, mineral matrix binding. Thus nanoindentation of remineralized dentin in water appears to be an improved method to assess the effectiveness of remineralization treatments.

Results showed that higher crystal growth rates (*R*) do not necessarily yield higher mechanical recovery, particularly in subsurface areas. The results of the present study, in agreement with previous reports (Bertassoni et al., 2009; Kinney et al., 2003a), support this hypothesis, showing that mechanical recovery of dentin in water not only depends on total mineral reformed, as indicated by the rates of crystal growth (R) here, but also the particular location and interaction of the mineral within the matrix.

Surface vs. cross section mechanical recovery

Our observations showed that DS=10.1 yielded significantly higher surface mechanical properties after 8 and 24 hours as compared to DS=9.8, nevertheless, surface properties were significantly lower than normal dentin. On the other hand, the cross-section measurements showed that both DS=10.1 and DS=9.8 yielded values generally not statistically different from each other in subsurface areas and eventually reached values of normal dentin. Interestingly only the surface properties correlated with *R* after remineralization, being significantly higher for the higher DS and presenting a slight increase with time for both groups (except DS=10.1 at 24 hrs). This was not observed in the cross-section measurements. These results suggest that while surface mechanical recovery was more dependent on the total content of mineral in the tissue (the higher the *R*, the higher recovery), recovery of the inner regions was more reliant upon the appropriate mineral matrix binding, and for this reason the higher *R* of group DS=10.1 yielded a similar recovery to the lower *R* of group DS=9.8.

The gradual mechanical recovery

Cross-section measurements of the demineralized dentin showed that the outer portions of the lesions had lower E_r, increasing gradually inwards, thus suggesting that the mineral was gradually removed as the acid diffused through the matrix, as expected (Zheng et al., 2003). Recent studies have shown that the extrafibrillar mineral is dissolved much more rapidly than the intrafibrillar mineral (Balooch et al., 2008). Thus, deeper areas should contain more mineral, particularly intrafibrillarly, for subsequent nucleation and growth during

remineralization. This is supported by the gradual increase in properties from the innermost regions outwards we observed. These observations are in agreement with a previous study (ten Cate, 2001) which reported mineral deposition at the innermost parts of lesions moving outwards over time. It was proposed that if precipitation is 'slow', a constant concentration of calcium and phosphate is maintained with depth in the matrix, thus, the rate of mineral deposition depends on the precipitation kinetics (ten Cate, 2001). The similar mechanical recovery between the treatment groups found in the cross-section analyses of the current study suggested that mechanical recovery occurred as long as the remineralizing solutions were in a metastable range, thus allowing for a continuous and relatively slow mineral growth. Thus, under the conditions studied, we suggest that intrafibrillar remineralization appears to be a more 'nucleation' dependent rather than 'precipitation'-controlled mechanism. Yet, more studies are necessary to better understand the thermodynamic mechanisms underlying intrafibrillar remineralization. We also add that visualization of the steps leading to intrafibrillar remineralization will be crucial to confirm the mechanisms proposed herein, and the association of mechanical recovery data together with microscopy techniques, such as the ones reported by Gu and colleagues (Gu et al, 2010) and more recently by Bertassoni et al (Bertassoni et al, 2010) appears to be a valuable tool to be applied in future remineralization studies.

The heterogeneous pattern of mechanical recovery

Interestingly, the 8 hour E_r for the group DS=9.8 near the surface was lower than at 4 hours. This is explained by the analyses of isolated indentation lines (Fig. 4) that consistently showed a heterogeneous pattern of mechanical recovery, meaning that for the same specimens areas of full mechanical recovery were found only 3 μm distant from areas where properties were very low. Such a heterogeneous pattern appeared to vanish with time, thus it appears that remineralization occurs via formation of remineralized islands that tend to grow in size and eventually link up, forming a more homogeneously remineralized tissue, as graphically depicted in the sequence shown in figures 4d, 4e and 4f. Interestingly, these results suggest that remineralization might occur similarly to dentinogenesis, where multiple globular mineral foci, known as calcospherites, grow and coalesce to form a relatively uniform mineralization front. The heterogeneous pattern that we observed could also be related to the presence of the so-called "globular dentin" or the "Tomes granular layer" in the root dentin, which are spots where adjacent calcospherites fail to link up, rendering to the tissue its granular appearance. In this case de- and remineralization should recreate the heterogeneous pattern. Additionally, formation of calcium phoshpate mineral phases on collagen type I (Combes et al., 1999) and using the constant solution composition (Wang and Nancollas, 2008) have been reported to obey a polynucleation mechanism, thus yielding a similar pattern as the one observed in this study.

Steps leading to remineralization of dentin at the nano- and micro-structural levels – a proposed model

Although the focus of this study is on mechanical recovery we propose a model that attempts to explain the steps involved in the de- and remineralization of dentin at the nano and micro-structural levels. Initially the fibrils present intrafibrillar and extrafibrillar mineral fully covering their structure, thus yielding high properties to the tissue (Fig 5a). With initial demineralization the extrafibrillar mineral is more rapidly dissolved (Balooch et al., 2008) (Fig 5b-c); at this stage much of the intrafibrillar mineral should remain (Fig 5c) and the properties should be substantially lower than normal. With further mineral loss, the intrafibrillar mineral is partially dissolved, and the gap zones become more visible (Fig 5d) (Balooch et al., 2008). If demineralization continues, the fibril will eventually be fully demineralized (Fig 5e) and properties should be very low. If demineralization stops some intrafibrillar mineral crystallites should remain and act as nucleation sites for

remineralization to occur (Fig 5f). After intrafibrillar nucleation the mineral grows and eventually fills the collagen fibril (Fig 5g), thus reinforcing its inner structure and yielding increased properties. With further growth the mineral coats the collagen and re-covers its external surface as extrafibrillar mineral (Fig 5h) providing full mechanical recovery.

5. Conclusion

In summary, we found mechanical recovery of hydrated artificial dentin carious lesions after remineralization with calcium and phosphate solutions. Our findings suggest that, at a macro-scale, remineralization might initiate heterogeneously and move towards a more homogenous pattern with time. Results also demonstrate that remineralization occurs primarily within deeper areas of the lesions, due to increased presence of remnant mineral foci, proceeding outwards with time. Additionally, results suggest that, at a micro-scale, remineralization may be dependent on remnant intrafibrillar mineral nuclei within the collagen, which are expected to be most prevalent in deeper and less demineralized zones of carious dentin.

Acknowledgments

References

1. Angker L, Nijhof N, Swain MV, Kilpatrick NM. Influence of hydration and mechanical characterization of carious primary dentine using an ultra-micro indentation system (UMIS). European Journal of Oral Sciences. 2004; 112:231–6. [PubMed: 15154920]

2. Arends J, Ruben JL, Inaba D. Major topics in quantitative microradiography of enamel and dentin: R parameter, mineral distribution visualization, and hyper-remineralization. Advances in Dental Research. 1997; 11:403–14. [PubMed: 9470497]

3. Balooch M, Habelitz S, Kinney JH, Marshall SJ, Marshall GW. Mechanical properties of mineralized collagen fibrils as influenced by demineralization. Journal of Structural Biology. 2008; 162:404–10. [PubMed: 18467127]

4. Bembey AK, Bushby AJ, Boyde A, Ferguson VL, Oyen ML. Hydration effects on the micro-mechanical properties of bone. Journal of Materials Research. 2006a; 21:1962–1968.

5. Bertassoni LE, Habelitz S, Kinney JH, Marshall SJ, Marshall GW Jr. Biomechanical perspective on the remineralization of dentin. Caries Research. 2009; 43:70–7. [PubMed: 19208991]

6. Bertassoni LE, Habelitz S, Pugach M, Soares PC, Marshall SJ, Marshall GW Jr. Evaluation of Surface Structural and Mechanical Changes Following Remineralization of Dentin. Scanning. 2010 in press.

7. Combes C, Rey C, Freche M. In vitro crystallization of octacalcium phosphate on type I collagen: influence of serum albumin. Journal Material Sciences: Materials in Medicine. 1999; 10:153–60.

8. Doerner MF, Nix WD. A method for interpreting the data from depth-sensing indentation instruments. Journal Material Research. 1986; 1:601–609.

9. Gu LS, Huffman BP, Arola DD, Kim YK, Mai S, Elsalanty ME, Ling JQ, Pashley DH, Tay FR. Changes in stiffness of resin-infiltrated demineralized dentin after remineralization by a bottom-up biomimetic approach. Acta Biomaterialia. 2010; 6:1453–61. [PubMed: 19887126]

10. He LH, Swain MV. Influence of environment on the mechanical behaviour of mature human enamel. Biomaterials. 2007; 28:4512–20. [PubMed: 17659336]

11. Katz EP, Li ST. Structure and function of bone collagen fibrils. Journal Molecular Biology. 1973; 80:1–15.

12. Kinney JH, Habelitz S, Marshall SJ, Marshall GW. The importance of intrafibrillar mineralization of collagen on the mechanical properties of dentin. Journal of Dental Research. 2003a; 82:957–61. [PubMed: 14630894]

13. Koutsoukos P, Amjad Z, Tomson MB, Nancollas GH. Crystallization of Calcium Phosphates - Constant Composition Study. Journal of the American Chemical Society. 1980; 102:1553–1557.

14. Landis WJ, Song MJ, Leith A, Mcewen L, Mcewen BF. Mineral and Organic Matrix Interaction in Normally Calcifying Tendon Visualized in 3 Dimensions by High-Voltage Electron-Microscopic Tomography and Graphic Image-Reconstruction. Journal of Structural Biology. 1993; 110:39–54. [PubMed: 8494671]

15. Larsen, MJ. Ion Products and Solubility of Calcium Phosphates. Denmark: Royal Dental College; 2001.

16. Marshall GW, Habelitz S, Gallagher R, Balooch M, Balooch G, Marshall SJ. Nanomechanical properties of hydrated carious human dentin. Journal of Dental Research. 2001; 80:1768–71. [PubMed: 11669491]

17. Marshall GW Jr, Marshall SJ, Kinney JH, Balooch M. The dentin substrate: structure and properties related to bonding. Journal of Dentistry. 1997; 25:441–58. [PubMed: 9604576]

18. McIntyre JM, Featherstone JD, Fu J. Studies of dental root surface caries. 1: Comparison of natural and artificial root caries lesions. Australian Dental Journal. 2000; 45:24–30. [PubMed: 10846269]

19. Oliver WC, Pharr GM. An Improved Technique for Determining Hardness and Elastic-Modulus Using Load and Displacement Sensing Indentation Experiments. Journal of Materials Research. 1992; 7:1564–1583.

20. Oyen ML. Poroelastic nanoindentation responses of hydrated bone. Journal of Materials Research. 2008; 23:1307–1314.

21. Rahiotis C, Vougiouklakis G. Effect of a CPP-ACP agent on the demineralization and remineralization of dentine in vitro. Journal Dentistry. 2007; 35:695–8.

22. Rho JY, Pharr GM. Effects of drying on the mechanical properties of bovine femur measured by nanoindentation. Journal Materials Sciences: Materials in Medicine. 1999; 10:485–8.

23. Saito T, Yamauchi M, Crenshaw MA. Apatite induction by insoluble dentin collagen. Journal of Bone Mineral Research. 1998; 13:265–70.

24. Shibata Y, He LH, Kataoka Y, Miyazaki T, Swain MV. Micromechanical property recovery of human carious dentin achieved with colloidal nano-beta-tricalcium phosphate. Journal of Dent Research. 2008; 87:233–7.

25. Tay FR, Pashley DH. Guided tissue remineralisation of partially demineralised human dentine. Biomaterials. 2008; 29:1127–37. [PubMed: 18022228]

26. ten Cate JM. Remineralization of caries lesions extending into dentin. Journal of Dental Research. 2001; 80:1407–1411. [PubMed: 11437209]

27. Tomson MB, Nancollas GH. Mineralization Kinetics: A Constant Composition Approach. Science. 1978; 200:1059–1060. [PubMed: 17740700]

28. Vollenweider M, Brunner TJ, Knecht S, Grass RN, Zehnder M, Imfeld T, et al. Remineralization of human dentin using ultrafine bioactive glass particles. Acta Biomaterialia. 2007; 3:936–943. [PubMed: 17560183]

29. Wang LJ, Nancollas GH. Calcium Orthophosphates: Crystallization and Dissolution. Chemical Reviews. 2008; 108:4628–4669. [PubMed: 18816145]

30. Zheng L, Hilton JF, Habelitz S, Marshall SJ, Marshall GW. Dentin caries activity status related to hardness and elasticity. Eur J Oral Sci. 2003; 111:243–52. [PubMed: 12786956]
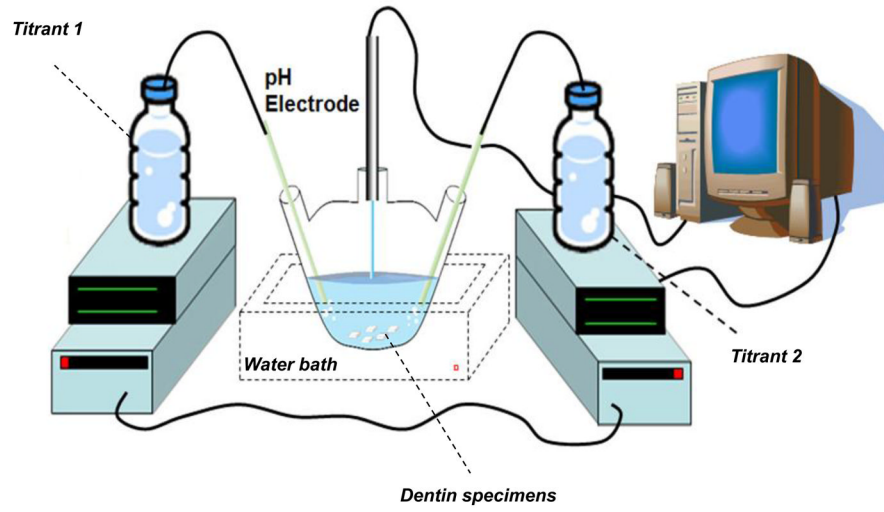
Figure 1.
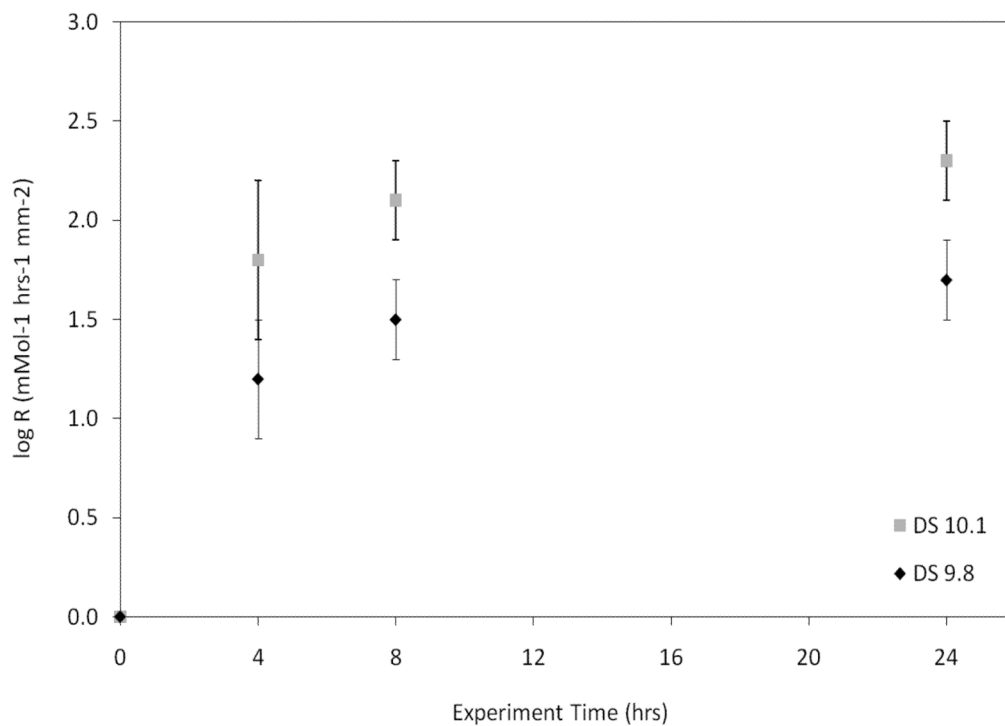Illustration of the constant composition system.

Figure 2.
Rates of crystal growth obtained from experiments with DS=10.1 and 9.8. Growth rates (*R*) were higher for DS=10.1 and increased with time for both groups. The increase became less significant at each time point.
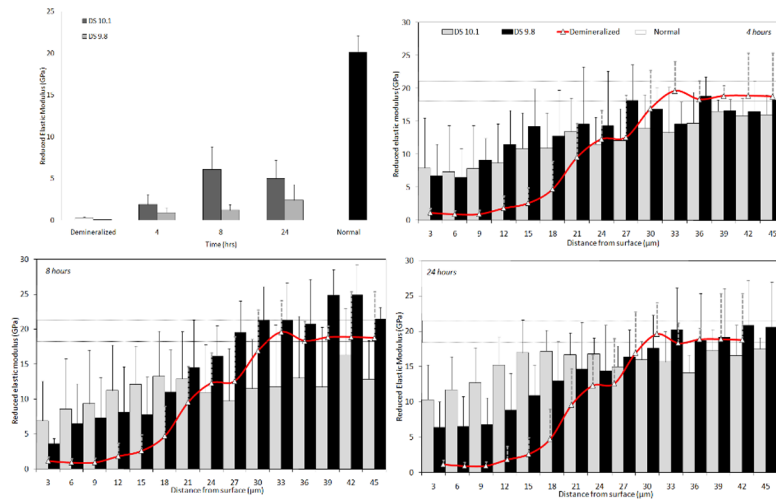
Figure 3.
Values of reduced elastic modulus (E_r) obtained from surface (a) and cross-section measurements after 4 (b), 8 (c) and 24 hours (d) from remineralization treatments for groups DS=10.1 and DS=9.8.
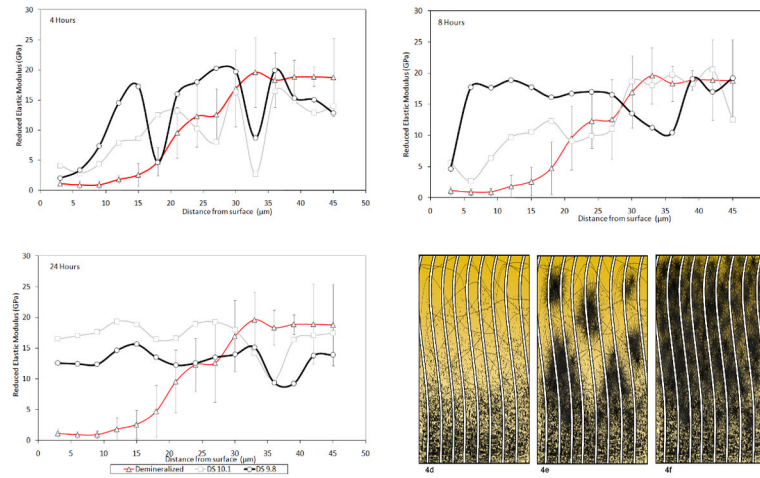
Figure 4.
Representative data obtained from one line of cross-section measurements from one single specimen at different time points. At 4 hours a heterogeneous pattern of mechanical recovery is noticed (a). The differences in properties decrease after 8 hours (b) and become more homogeneous at 24 hours (c). The schematic represents hypothetical steps for remineralization at a micro-scale: (d) after demineralization, (e) during the formation of "growth units", and finally (f) having a relatively homogeneous remineralization.
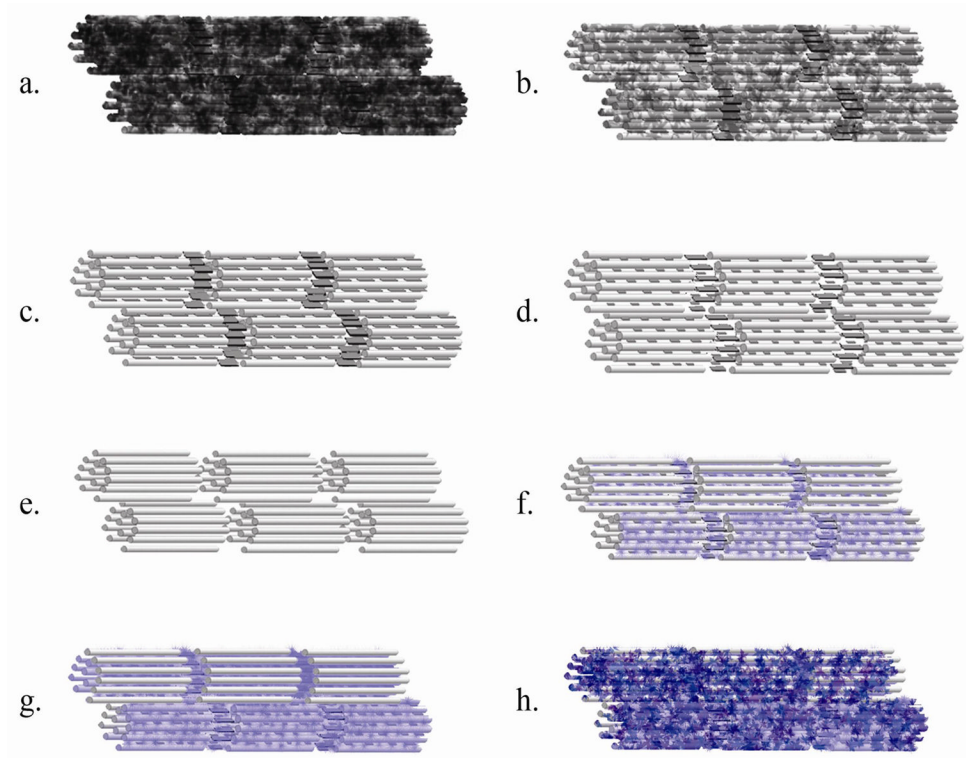
Figure 5.
Steps involved on de- and remineralization of collagen fibrils of dentin at a nano-scale. Dark 'crystals' are mineral present before acid attack and blue 'crystals' are re-grown mineral.

Table 1

Experimental conditions and groupings. $CaCl_2$ and KH_2PO_4 concentrations in the reaction vessel are shown as averaged values of measurements at 4, 8 and 24 hours for a 200 ml volume.

Group	pH		Reaction vessel (mM)			Titrant 1 (mM)		Titrant 2 (mM)	
DS_{HAP}			$[CaCl_2]$	$[KH_2PO_4]$		$[CaCl_2]$	$[KCl]$	$[KH_2PO_4]$	$[KOH]$*
10.1	7.4	0.05	1.6	0.11	1.1	0.16	8.2	284	5.2	11.8
9.8	7.4	0.05	1.2	0.04	0.72	0.03	7.4	284	4.5	10.3